Pis'ma v ZhETF, vol. 98, iss. 11, pp. 776 – 781

On triggering role of carrier mobility for Laughlin state organization

J. Jacak[*1)], *L. Jacak*[*]

[*] *Institute of Physics, Wrocław University of Technology, 50-370 Wrocław, Poland*

Submitted 26 August 2013

Recent experiments with suspended graphene have corroborated an important role of carrier mobility in the competition between Laughlin state and insulating state, presumably of Wigner-type electron crystal. Moreover, the fractional quantum Hall effect (FQHE) in graphene has been observed at low carrier densities when the interaction was reduced due to carrier dilution. This suggests that not solely interaction and the flat band with quenched kinetic energy may be important for formation of FQHE. Here, some exclusive for 2D topological arguments are supposed to explain the triggering role of carrier mobility in formation of the collective FQHE state, when conditions of sufficient flattening of a band and interaction presence are fulfilled.

DOI: 10.7868/S0370274X13230094

1. Introduction. Fractional quantum Hall effect (FQHE) is the major example of strongly correlated electron states in confined geometry, which manifest itself in 2D charged systems at the presence of quantizing magnetic field at specific fractional fillings of Landau levels (LLs). In its essentially collective character the primary role plays interaction in the case when kinetic energy is inactivated by flattening of a band, like for massive ideal degeneration of Landau levels in the case of noninteracting particles only slightly blurred by interaction. The corresponding correlations are expressed in the form of famous Laughlin wave function [1] which corresponds [2, 3] to an exact ground state for 2D system of charged particles in the presence of magnetic field at the lowest LL filling $1/p$ (p-odd), when the short range part of Coulomb interaction is included. This has been demonstrated using the so-called Haldane pseudopotentials, i.e., matrix elements of Coulomb interaction in the basis of relative angular momenta m of electron pairs. The short range part of the interaction is assumed to be limited to the first $m = p-2$ Haldane terms (suitably for the p-th fractional state) and it has been verified that the long range tail with $m > p-2$ did not influence significantly this state [3]. Occurrence of FQHE at only certain filling fractions – the simplest one equals 1/3 – is a mysterious property of correlations not satisfactory elucidated as of yet, though illustrated by some auxiliary effective models like composite fermion (CF) concept. The idea of CFs is very attractive as it offers a simple single-particle effective description of highly correlated multi- particle state. However, the cost of this simplification is heuristic introduction of auxiliary magnetic field flux tubes associated to electrons [4]. $p-1$ flux quanta tube each fixed somehow to electrons change the particle correlations suitably to requirements of the Laughlin function due to phase shift of Aharonow–Bohm-type when CFs mutually exchange positions. The success of CF model follows from its ability to predict FQHE hierarchy via single-particle argument that for fractional fillings a resultant magnetic field of external field and of averaged field of flux-tubes coincide with field value when integer quantum Hall effect (IQHE) occurs. Note, however, that some experimentally observed fractions for FQHE (5/13 and 4/11) are out of this hierarchy (given by $\nu = \frac{n}{n(p-1)\pm 1}$, p odd integer, n integer) and need some other explanation. The CFs are assumed as weakly residually interacting effective particles thus often treated as a sort of quasiparticles. The CF concept can be also supported by Chern–Simons singular gauge field approach in the form of formalism suitable to efficient calculations resulting in a good agreement with exact diagonalizations, especially inside the lowest LL [5, 6].

Recent experimental investigation of FQHE in graphene [7, 8] have shed, however, new light on this correlated state and seem to go beyond ability of explanation concentrated solely on the interaction and band flattening. Moreover, by presumption that the local flux-tubes of CFs are a result of the interaction [5, 6] one would lose important topological argument which may explain the origin of effective CF structure with its heuristic auxiliary elements.

Some hints can be taken from recent demonstration in graphene [7] consisting in observation of FQHE in the same sample of so called suspended graphene and upon the same conditions but only after the annealing process

[1)] e-mail: janusz.jacak@pwr.wroc.pl

enhancing carriers mobility while not changing interaction. Before annealing, the state at 1/3 filling was insulating (conjectured as of Wigner crystal type), while after annealing without changing other conditions the FQHE has occurred. This complies also with requirements of high carriers mobility needed for observation of FQHE in traditional semiconductor heterostructures which was earlier evidenced [9].

In the present letter we revisit the foundations of the CF model and supply topological arguments in agreement with recent observations in graphene, thereby highlighting the triggering role of the carrier mobility in FQHE formation.

2. FQHE in graphene–description of experimental results. *Short summarizing of graphene structure.* The hexagonal 2D structure of graphene with two carbon atoms per unit cell results in a double triangular lattice arranged in a honeycomb pattern. The carbon p orbitals perpendicular to the plane hybridize to type π states of the band structure well described in the approximation of the strong coupling, $E_{\pm}(\mathbf{k}) = \pm t\sqrt{3+f(\mathbf{k})} - t'f(\mathbf{k})$, where $f(\mathbf{k}) = 2\cos(\sqrt{3}k_y a) + 4\cos\left(\frac{\sqrt{3}}{2}k_y a\right)\cos\left(\frac{3}{2}k_x a\right)$, $a \simeq 0.142\,\mathrm{nm}$ is distance between carbon atoms, $t = 2.7\,\mathrm{eV}$ – hopping energy to the nearest neighbors (between sublattices), $t' = 0.2t$ – hopping energy to next-nearest neighbors (inside the sublattices). The valence band and the conduction band meet in points called K and K' at the border of a hexagonal Brillouin zone [10, 11] in compliance with the above relation for $t' = 0$. Both bands met in these points (non-gap semiconductor) have locally a conical shape, which results in local linear relation between energy and momentum formally equivalent to that of relativistic fermions with zero rest mass ($E = \pm\sqrt{m_0^2 v_F^4 + p^2 v_F^2}$, with $m_0 = 0$), described by Dirac equation but with the velocity of light replaced by the Fermi velocity, $v_F \simeq c/300$ [11, 12], $-iv_F\boldsymbol{\sigma}\cdot\nabla\Psi(\mathbf{r}) = E\Psi(\mathbf{r})$ (Pauli matrices correspond to the pseudospin structure related to two sublattices) [11, 13]. The zero mass of the Dirac fermions leads to numerous consequences and electron anomalies in the properties of graphene [11, 13–15]. For Dirac particles with zero rest mass, momentum uncertainty also leads to energy uncertainty (contrary to non-relativistic case), which results in the time evolution mixing together particle states with hole (antiparticle) states for relativistic type dynamics. For zero-mass Dirac electrons the scaling of cyclotron energy is different as well ($\sim B^{1/2}$, and not $\sim B$, as in the case of non-relativistic particles). The value of this energy is also different, and larger by far (two orders of magnitude larger than the one corresponding in classical materials, i.e., it is (due to zero mass in Dirac point) as much as about 1000 K, for 10 T field), which allows to observe the IQHE in graphene even at room temperatures [14, 15]. There is, however, an anomalous IQHE observed here (for $\nu = \pm 4(n+1/2)$, or for $\pm 2, \pm 6, \pm 10, \ldots$ and at zero Landau level in the Dirac point, i.e., for zero energy; $\pm$ corresponds to particles and holes, respectively, 4 results from pseudospin/valley degeneration, 1/2 is associated with Berry's phase for pseudospin) [11–16]. The Klein paradox, referring to ideal tunneling of Dirac particles by rectangular potential barriers leads to extensive mobility of charge carriers in graphene, which is experimentally observed even near Dirac point (Fermi level at the border between electrons and holes). In this point, the density of charges is zero (and the zero Landau level is located here, employing both bands) [11, 14, 15, 12].

Searching for FQHE in grapheme. Despite using very strong magnetic fields (up to 45 T), FQHE was not detected initially in graphene samples deposited on a substrate of SiO_2 [17]. In [17] it was noted, however, the emergence of additional plateaus of IQHE for the fillings $\nu = 0, \pm 1, \pm 4$, indicating the elimination of spin-pseudospin degeneration (related to sublattices), as a result of increasing mass of Dirac fermions [17]. Only after mastering the novel technique of the so-called suspended ultra-small graphene scrapings with extreme purity and high mobility of carriers (beyond $2\cdot 10^5\,\mathrm{cm^2\cdot V^{-1}\cdot s^{-1}}$; note that high mobility is necessary also to observe the FQHE in the case of semiconductor 2D hetero-structures, and reaches there even higher values of millions $\mathrm{cm^2\cdot V^{-1}\cdot s^{-1}}$ [9]), it was possible to observe the FQHE in graphene at fillings $\nu = 1/3$ and $-1/3$ (the latter for holes, with opposite polarization of the gate voltage, which determines Fermi level position, either in the conduction band, or in the valence band) [7, 8]. Both papers [7, 8] report the observation of the FQHE in graphene, in the paper [8], in a field of 12–14 T, for electron concentration of $10^{11}\,\mathrm{cm^{-2}}$ (the mobility of $25\cdot 10^4\,\mathrm{cm^2\cdot V^{-1}\cdot s^{-1}}$) and in the paper [7], in a field of 2–12 T, but for a concentration level smaller by one order of magnitude ($10^{10}\,\mathrm{cm^{-2}}$ and the mobility of $2\cdot 10^5\,\mathrm{cm^2\cdot V^{-1}\cdot s^{-1}}$).

The FQHE in suspended graphene has been observed at the temperatures around 10 K [18], and even higher (up to 20 K) [19]. Authors of the paper [19] have argued that the critical temperature elevation is related to the stronger electric interaction caused by the lack of a dielectric substrate (with a relatively high dielectric constant in case of semiconductors, ~ 10) in the case of suspended samples. However, some aspects that are likely more important are the high mobility value (with suppressed acoustic phonon interaction in ideal 2D system, in comparison to 3D substrate) and, on the other hand, the very high cyclotron energy in graphene (i.e., the large energy gap between the incompressible states).

In the papers [15, 16] the competition between the FQHE state with the insulator state near the Dirac point has also been demonstrated, corresponding to a rapidly decreasing carrier concentration (and thus reducing interaction role at larger separation of carriers), Fig. 1. The most intriguing observation is that one [7]

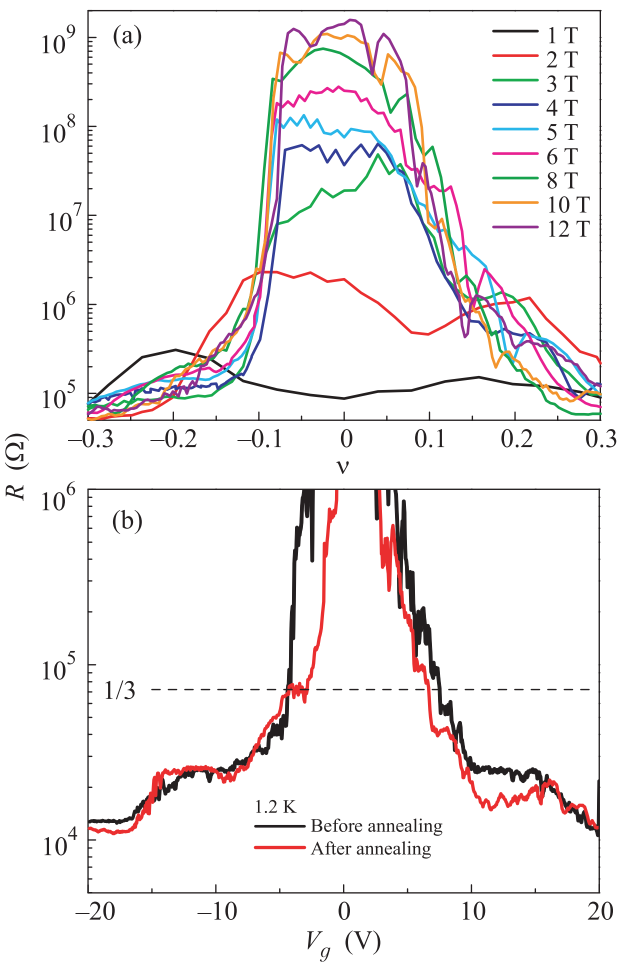

Fig. 1. (a) – The emergence of an insulator state accompanying the increase in the strength of a magnetic field around the Dirac point. (b) – Competition between the FQHE and the insulator state for the filling $-1/3$: annealing removes pollution which enhances the mobility and provides conditions for the emergence of a *plateau* indicating the FQHE [7]

demonstrating an influence of annealing – in Fig. 1 it is shown that FQHE occurs in the same sample originally insulating, upon same conditions, but after the annealing process enhancing mobility of carriers due to impurities and defects reduction. This demonstrates directly the triggering role of carriers mobility in FQHE state arrangement. It should be added that very recent progress in the experiment allows also for observation of FQHE in graphene on the BN substrate in large magnetic fields of order of 40 T (remarkably, FQHE features were noticed up to fourth Landau level, which is the record with this regard) [20].

3. Quasiclassical quantization of the magnetic field flux for composite fermions. The topological arguments with regard to 2D charged multi-particle systems at presence of strong magnetic field were developed in [21, 22]. The main related aspects are as follows. 1) At fractional fillings of the LLL classical cyclotron orbits are *too short* for particle exchanges in the picture of braid groups (note that this is no case in 3D where long range helical motion allows reaching even distant particles). 2) Particle exchanges are necessary to create a collective state such as the FQHE – thus the cyclotron radius must be enhanced somehow, and indeed in the model of CFs [4] this enhancement is achieved by adding flux tubes directed oppositely to the external field and reducing resultant field strength. 3) A natural way to enhance cyclotron radius is, however, by use of multi-looped cyclotron trajectories related to multi-looped braids that describe elementary particle exchanges (the resulting cyclotron braid subgroup is generated by σ_i^p, $i = 1, ..., N$, σ_i are generators of the full braid group) – in 2D all loops of multi-looped trajectory must share together the same total external magnetic field flux and this is a reason of enhancement of all loops dimensions effectively fitted accurately to particle separation at LLL fillings $1/p$, (p-odd). This is in contrast to 3D where each additional loop adds in fact a surface and rises total flux of field passing through all loops as e.g., in 3D solenoid. 4) In accordance with the rules of path integration for non-simply-connected configuration spaces [23], one-dimensional unitary representations (1DURs) of a corresponding braid group define the statistics of the collective system. In the case of multi-looped braids, naturally assembled into the cyclotron subgroup instead of the full braid group, one arrives in this way at the statistical properties required by the Laughlin correlations (1DURs are here $\sigma_i^p \to e^{ip\alpha}$, $\alpha \in [0, 2\pi)$, CFs correspond to the choice $\alpha = \pi$). 5) The interaction is crucial for properly determining the cyclotron braid structure because its short range part prevents the particles from approaching one another closer than the distance given by the density.

The listed points are summarized in Fig. 2 (for details cf. Refs. [22, 24]).

The above topological braid group argumentation explains the usefulness of fictitious auxiliary elements

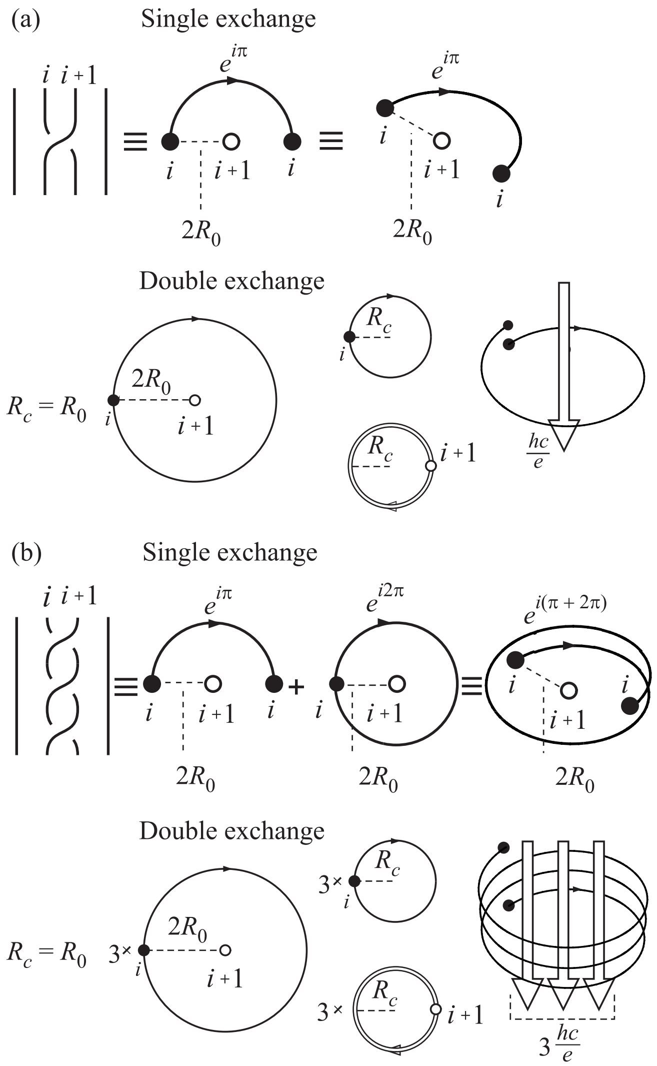

Fig. 2. The braid generator corresponds to the exchange of neighboring particles along half of cyclotron trajectories of individual particles (the relative trajectory is drawn), while the closed cyclotron orbits of individual particles result in the double exchange. (a) – For $\nu = 1$ when single-looped cyclotron trajectory reaches neighboring particles, $R_c = R_0$. (b) – For $\nu = 1/3$ with additional two loops needed for $R_c = R_0$ (R_c is an effective cyclotron radius, $2R_0$ is the particle separation; each loop of individual particle cyclotron orbit encircles quantum of external magnetic field flux, hc/e; third dimension added for better visualization)

of CFs, i.e., of mysterious flux tubes, and proves that CFs are not quasiparticles dressed with fluxes due to interaction (like familiar from condensed matter Landau quasiparticles), but are rightful quantum 2D particles assigned with Laughlin statistics determined by 1DURs of the appropriate cyclotron braid subgroup.

The wave packets corresponding to the carrier dynamics are related to the collective character of a multiparticle system. For LLL of noninteracting system the group velocity of any packet is zero due to degeneration of states. Interaction removes, however, this degeneracy and provides packet dynamics. The collective movement minimizes kinetic energy, whereas the interaction favors localization (localization causes increase in kinetic energy). Therefore, the collectivization prefers movement of carriers along accessible trajectories – periodic and closed as a rule at the magnetic field presence [25], which then must, however, embrace quantized external magnetic field fluxes. This is a role for collectivization in the energy preference of wave packets traversing closed trajectories in correspondence with the classical cyclotron braid group description. This appears to be in accordance with the FQHE observations in graphene, which are found also at a surprisingly low carrier density at which dilution reduced interaction usually treated as prerequisite for fractional collective state. However, lower density corresponds to larger interparticle separations and then larger cyclotron orbits fit to these distances, what agrees with observation of FQHE at relatively lower fields [7, 8].

Carrier mobility refers also to quasiclassical wave packet dynamics in terms of the drift velocity in an electric field and the classical Hall effect which can reflect various scattering phenomena including their effective characteristic by mobility of carriers (the mobility $\mu \sim \lambda$, where λ is the mean free path). The topological arguments in the 2D case lead to preference of higher mobility as longer mean free path is required for wave packets to traverse multi-looped trajectories.

Cyclotron braid group approach to FQHE in grapheme. From the cyclotron braid group point of view, the experimental observations of FQHE in graphene [7, 8] seem to be compliant with the expectations of the braid description. In the case of graphene, controlling lateral gate voltage (within the range up to 10 V [8]) allows to separately adjust density of carriers at a constant magnetic field, which was no case in 2DEG in semiconductor heterostructures. For low concentration, while closing on the Dirac point, one may expect that too strong fields would exceed the stability threshold of the FQHE state in competition with the Wigner crystal, and that corresponds to the emergence of the insulating state near the Dirac point in a strong magnetic field (in standard 2DEG magnetic field corresponding to $\nu \simeq 1/9$ destabilizes FQHE [6]). In the case of the hexagonal structure of graphene, electron (or hole) Wigner crystallization may exhibit interference between the triangular crystal sublattices, and inclusion of the resonance (hopping) between these two sublattices may cause blurring of the sharp transition to the insulator state, which seems compliant with the observations (Fig. 1). Some specific character of FQHE features in graphene would be also linked with spin-valley SU(4) symmetry of Dirac carriers [20, 26], but even though one can use the multicomponent model of FQHE suited to SU(4) symmetry, in the form of the Halperin wave function [27, 28], the components of this function have Jastrow polynomial form, and the similar topological interpretation still holds as in the single component electron liquid.

The carrier mobility in suspended graphene reaches $250000\,\mathrm{cm}^2\cdot\mathrm{V}^{-1}\cdot\mathrm{s}^{-1}$. Let us note that this value is lower than the record one for semiconductor 2D structures, being ca. $30\cdot 10^6\,\mathrm{cm}^2\cdot\mathrm{V}^{-1}\cdot\mathrm{s}^{-1}$ [9]. Nevertheless, the corresponding mean free path in both cases, in suspended graphene and in traditional 2DEG semiconductor systems manifesting FQHE presence, well exceeds the sample dimensions (typically of μm order) [9, 29]. The mean free path exceeding sample size corresponds, upon the cyclotron braid approach, to possibility of realization of more complicated braids (i.e., not only of group generators but also of their products), which in magnetic field allow carriers to traverse edge-to-edge pathways by series of cyclotron exchanges and collisions in equidistantly distributed particle web blocked by Coulomb interaction, resulting in conducting collective state. This emphasizes the central role of Coulomb repulsion in conducting FQH state formation but also the significance of the requirement of sufficiently long mean free path of carriers. Taking into account that cyclotron orbits must be p-looped in order to reach neighboring particles at LLL filling $1/p$, and to allow the series of exchanges needed to edge-to-edge pathways, the resulting mean free path should be p times longer than sample size, which fits with experimental observations both in the graphene [29] and semiconductor heterostructures [9].

4. Comment. Although particularities of real dynamics of quasiclassical wave packets represented carriers including their scattering on structure imperfections are beyond the ability of standard FQHE description, some general qualitative conclusions regarding topological specific character of dynamics in 2D can be drawn out. In the case of magnetic field corresponding to fractional fillings of the LLL, classical cyclotron orbits of electrons are shorter in comparison to particle separation. This prohibits particle exchanges in the braid group picture, in which these exchanges must be along cyclotron orbits at magnetic field presence. Single-looped trajectories are not effective in such system and must be excluded from path integral domain. Simultaneously, p-looped trajectories attain in 2D (with mag. field) larger size which accurately fits the interparticle distances at $\nu = 1/p$, p odd. But the multi-looped quasiclassical wave packet orbits with larger radii strongly favor higher mobility of carriers proportional to mean free path for carriers and this has been confirmed experimentally in suspended graphene. Reducing of structure imperfections by annealing of graphene sample indicated that the enhancement of mean free path and thus the growth of carrier mobility conditions forming of FQHE state.

Supported by Polish National Center of Science Project no: DEC-2011/02/A/ST3/001

1. R. B. Laughlin, Phys. Rev. Lett. **50**, 1395 (1983).
2. F. D. M. Haldane. Phys. Rev. Lett. **51**, 605 (1983).
3. R. E. Prange and S. M. Girvin, *The Quantum Hall Effect*, Springer Verlag, New York (1990).
4. J. K. Jain, Phys. Rev. Lett. **63**, 199 (1989).
5. O. Heinonen, *Composite Fermions*, World Sc., Singapore (1998).
6. J. K. Jain. *Composite Fermions*, Cambridge UP, Cambridge (2007).
7. K. I. Bolotin, F. Ghahari, M. D. Shulman, H. L. Störmer, and P. Kim, Nature **462**, 196 (2009).
8. X. Du, I. Skachko, F. Duerr, A. Luican, and E. Y. Andrei, Nature **462**, 192 (2009).
9. L. Pfeiffer and K. W. West, Physica E **20**, 57 (2003).
10. P. R. Wallace, Phys. Rev. **71**, 622 (1947).
11. A. H. Castro Neto, F. Guinea, N. M. R. Peres, K. S. Novoselov, and A. K. Geim, Rev. Mod. Phys. **81**(1), 109 (2009).
12. K. Yang, Sol. State Comm. **143**, 27 (2007).
13. A. K. Geim and A. H. MacDonald, Physics Today **8**, 35 (2007).
14. K. S. Novoselov, A. K. Geim, S. V. Morozov, D. Jiang, M. I. Katsnelson, I. V. Grigorieva, S. V. Dubonos, and A. A. Firsov, Nature **438**, 197 (2005).
15. Y. Zhang, Y.-W. Tan, H. L. Störmer, and F. Kim, Nature **438**, 201 (2005).
16. J. W. MacClure, Phys. Rev. **104**, 666 (1956).
17. Y. Zhang, Z. Jiang, J. P. Small, M. S. Purewal, Y.-W. Tan, M. Fazlollahi, J. D. Chudov, J. A. Jaszczak, H. L. Störmer, and P. Kim, Phys. Rev. Lett. **96**, 136806 (2006).
18. D. A. Abanin, I. Skachko, X. Du, E. Y. Andrei, and L. S. Levitov, Phys. Rev. B **81**, 115410 (2010).
19. I. Skachko, X. Du, F. Duerr, A. Luican, D. A. Abanin, L. S. Levitov, and E. Y. Andrei, Phil. Trans. R. Soc. A **368**, 5403 (2010).

20. C. R. Dean, A. F. Young, P. Cadden-Zimansky, L. Wang, H. Ren, K. Watanabe, T. Taniguchi, P. Kim, J. Hone, and K. L. Shepard, Nature Physics **7**, 693 (2011).
21. J. Jacak, I. Jóźwiak, and L. Jacak, Phys. Lett. A **374**, 346 (2009).
22. J. Jacak, I. Jóźwiak, L. Jacak, and K. Wieczorek, J. Phys: Cond. Matt. **22**, 355602 (2010).
23. M. G. Laidlaw and C. M. DeWitt, Phys. Rev. D **3**, 1375 (1971).
24. J. Jacak and L. Jacak, Europhys. Lett. **92**, 60002 (2010).
25. P. W. Eliutin and W. D. Krivchenkov, *Quantum Mechanics*, Nauka, Moscow (1976) (in Russian).
26. M. O. Goerbig, Rev. Mod. Phys. **83**, 1193 (2011).
27. B. I. Halperin, Helv. Phys. Acta **56**, 75 (1983).
28. M. O. Goerbig and N. Regnault, Phys. Rev. B **75**, 241405 (2007).
29. K. I. Bolotin, K. J. Sikes, Z. Jiang, M. Klima, G. Fudenberg, J. Hone, P. Kim, and H. L. Störmer, Solid State Comm. **146**, 351 (2008).